ARTICLE IN PRESS

Tetrahedron xxx (2018) 1–13

Contents lists available at ScienceDirect

Tetrahedron

journal homepage: www.elsevier.com/locate/tet

Ethynyl-bridged porphyrin-corrole dyads and triads: Synthesis, properties and DFT calculations

Baris Temelli*, Mine Gündüz, Dilek Yüksel

Hacettepe University, Department of Chemistry, Beytepe Campus, 06800, Ankara, Turkey

ARTICLE INFO

Article history:
Received 8 April 2018
Received in revised form
30 June 2018
Accepted 4 July 2018
Available online xxx

Keywords:
Porphyrin
Corrole
Sonogashira coupling
DFT

ABSTRACT

Ethynyl-bridged porphyrin-corrole dyads and triads were synthesized by using Pd(0) mediated coupling reactions and their structures were characterized by NMR, FT-IR, UV/Vis and fluorescence techniques. Besides spectroscopic techniques, computational studies at B3LYP/6-311G(d,p) level of DFT were also used to elucidate the minimum energy geometries and the molecular orbital characteristics of the new dyads and triads. DFT calculations pointed out the presence of charge separated donor-acceptor property between macrocycles of dyads and triads, and the emission studies indicated an excited state interaction between macrocycles, and energy transfer from the porphyrin to the corrole unit.

1. Introduction

Porphyrins are macrocyclic tetrapyrrolic aromatic compounds that play important roles in various metabolic systems such as oxygen and electron transfer [1]. Metal complexes of porphyrins are widely used in photodynamic therapy, dye-sensitized solar cells, and catalytic applications [2]. Multiporphyrin compounds have been the subject of intense research over the past few decades because of their applications in sensors, artificial photosynthetic systems and molecular wires [3]. However, these compounds consist of a single chromophore group that absorbs only particular wavelengths of the visible light. This limitation led to the use of porphyrin hybrid compounds with different chromophore groups such as, corroles [4], phythalocyanines [5], subporphyrins [6], bodipy [7] and expanded porphyrins [8]. The investigation of multi chromophore containing compounds and their excited state behaviors has made significant contributions to the applications on the conversion of solar energy into chemical energy. In this regard, corroles, contracted porphyrin analogs with direct pyrrole-pyrrole linkage, have attracted the attention due to their trianionic character, higher fluorescence quantum yields and lower oxidation potentials [9]. Although the applications of corroles as catalysts, sensors, and dye sensitized solar cells have received much attention, their integration into porphyrin hybrid compounds has remained limited. To date, only limited number of studies have reported on porphyrin-corrole conjugates and their applications have not been extensively studied. Smith and co-workers reported an approach to phenyl-linked porphyrin-corrole dyads *via* cyclization of phenyl-linked a,c-biladiene salts [4a]. Also, Kadish, Guillar and co-workers prepared metal complexes of cofacial porphyrin-corrole dyads, which are linked by anthracene, bipheylene, dibenzofuran, dibenzothiophene, dibenzofuran, dimethylxanthene, and diphenyl ether bridges [4b,c]. The amide connected porphyrin-corrole dyad was synthesized by Gryko and co-workers [4d]. Maes, Campagne and co-workers synthesized porphyrin-corrole conjugates through phenolic bond [4e]. Recently, click reaction was used to prepare zinc porphyrin-copper corrole dyads, triad and pentad [4f,g]. In addition, directly linked porphyrin-corrole hybrids were prepared by condensation reactions of formylated porphyrins [4h,i] and the Suzuki-Miyaura coupling of 2-boryl-substituted corrole [4j].

Though porphyrin-corrole conjugates have been connected by several linker groups, there is no report on the ethynyl linked example of these compounds. Very recently, we reported the synthesis and spectroscopic properties of imine-bridged [10] and directly-linked porphyrin-corrole dyads [11]. As a continuation of our studies on porphyrin-corrole conjugates, we present herein the investigation of the synthesis, some photo physical properties, and DFT calculations of meso-meso linked ethynyl-bridged porphyrin-corrole dyads and triads (Fig. 1).

---

* Corresponding author.
E-mail address: temelli@hacettepe.edu.tr (B. Temelli).

https://doi.org/10.1016/j.tet.2018.07.007
0040-4020/© 2018 Elsevier Ltd. All rights reserved.

Please cite this article in press as: B. Temelli, et al., Ethynyl-bridged porphyrin-corrole dyads and triads: Synthesis, properties and DFT calculations, Tetrahedron (2018), https://doi.org/10.1016/j.tet.2018.07.007

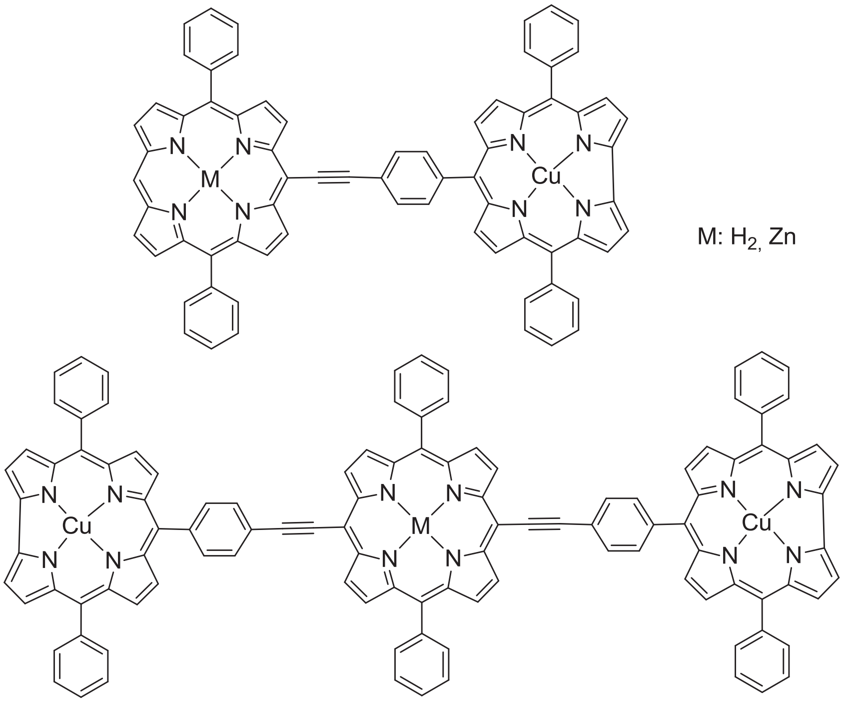

Fig. 1. Synthesized porphyrin-corrole dyads and triads.

2. Results and discussion

Sonogashira reactions of mono and bis ethynyl-substituted porphyrins with bromophenyl-substituted Cu(III) corrole complex were used to synthesize ethynyl-bridged dyads and triads. For corrole part of the conjugates, 10-(4-bromophenyl)-5,15-diphenylcorrole copper (III) (**3**) was synthesized in two steps according to the reported methods [12]. 10-(4-Bromophenyl)-5,15-diphenylcorrole (**2**) was prepared by the condensation of 5-phenyldipyrromethane (**1**) with 4-bromobenzaldehyde and subsequent oxidation of the reaction mixture with *p*-chloranil in $CHCl_3$. In the second step, 10-(4-bromophenyl)-5,15-diphenylcorrole (**2**) was converted to its Cu(III) complex in 89% yield (Scheme 1).

The synthesis of porphyrin part of the conjugates started with mono and dibromination of 5,15-diphenylporphyrin (**4**) by controlled addition of NBS. Mono brominated porphyrin **5** and dibrominated porphyrin **10** were isolated in 55% and 86% yields, respectively. Sonagashira reactions of porphyrins **5** and **10** with trimethylsilylacetylene at 80 °C in the presence of a catalytic amount of $PdCl_2(PPh_3)_2$ and CuI gave desired protected porphyrins **6** and **11**. After metalation reactions of *meso*-trimethylsillylethynyl substituted porphyrins with $Zn(OAc)_2$, TMS deprotections of both metal free porphrins (**6** and **11**) and Zn(II) porphyrin complexes (**7** and **12**) were carried out with TBAF in order to obtain *meso*-ethynyl-substituted porphyrins **8, 9**, **13,** and **14** (Scheme 2).

The metal free porphyrin-Cu(III) corrole dyad **15** and the triad **17** were synthesized under copper free Pd(0) coupling conditions at 40 °C with $Pd_2(dba)_3/AsPh_3$ catalyst. Reactions were monitored with TLC and the pure dyad **15** and the triad **17** were obtained after silica gel column chromatography in 64% and 48% yields respectively. For the synthesis of the Zn-porphyrin Cu(III)-corrole dyad **16** and the triad **18**, $PdCl_2(PPh_3)_2$/CuI catalyzed Sonogashira reaction protocol gave better yields than the copper free method. The dyad **16** was obtained in 68% yield, while the triad **18** was isolated in 40% yield after column chromatography (Scheme 3).

The structures of dyads and triads were identified by NMR and mass spectroscopy. The aromatic region of ^1H NMR spectrum of the dyad **15** and the comparison with those of its monomers **3** and **8** is shown Fig. 2. In dyad **15**, the resonances corresponding to the porphyrin and corrole subunits are present. *meso*-Proton of porphyrin subunit appeared at 10.31 ppm as a singlet. Although six β-porphyrin protons in dyad **15** (between 9.00 and 9.40 ppm) experienced slight downfield shifts compared with those of starting compound **8**, two β-porphyrin protons shifted upfield from 9.75 ppm to 9.38 ppm. The line-broadening, which affects corrole compounds, observed in corrole sub-unit **3**, disappeared in dyad **15** and β-protons of corrole subunit appeared at 7.74–7.78 ppm and 7.53–7.58 ppm as multiplets. Other signals in the spectrum of the

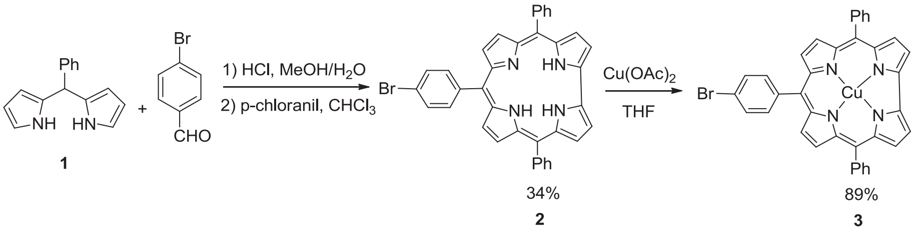

Scheme 1. Synthesis of 10-(4-bromophenyl)-5,15-diphenylcorrole copper (III) **3**.

Please cite this article in press as: B. Temelli, et al., Ethynyl-bridged porphyrin-corrole dyads and triads: Synthesis, properties and DFT calculations, Tetrahedron (2018), https://doi.org/10.1016/j.tet.2018.07.007

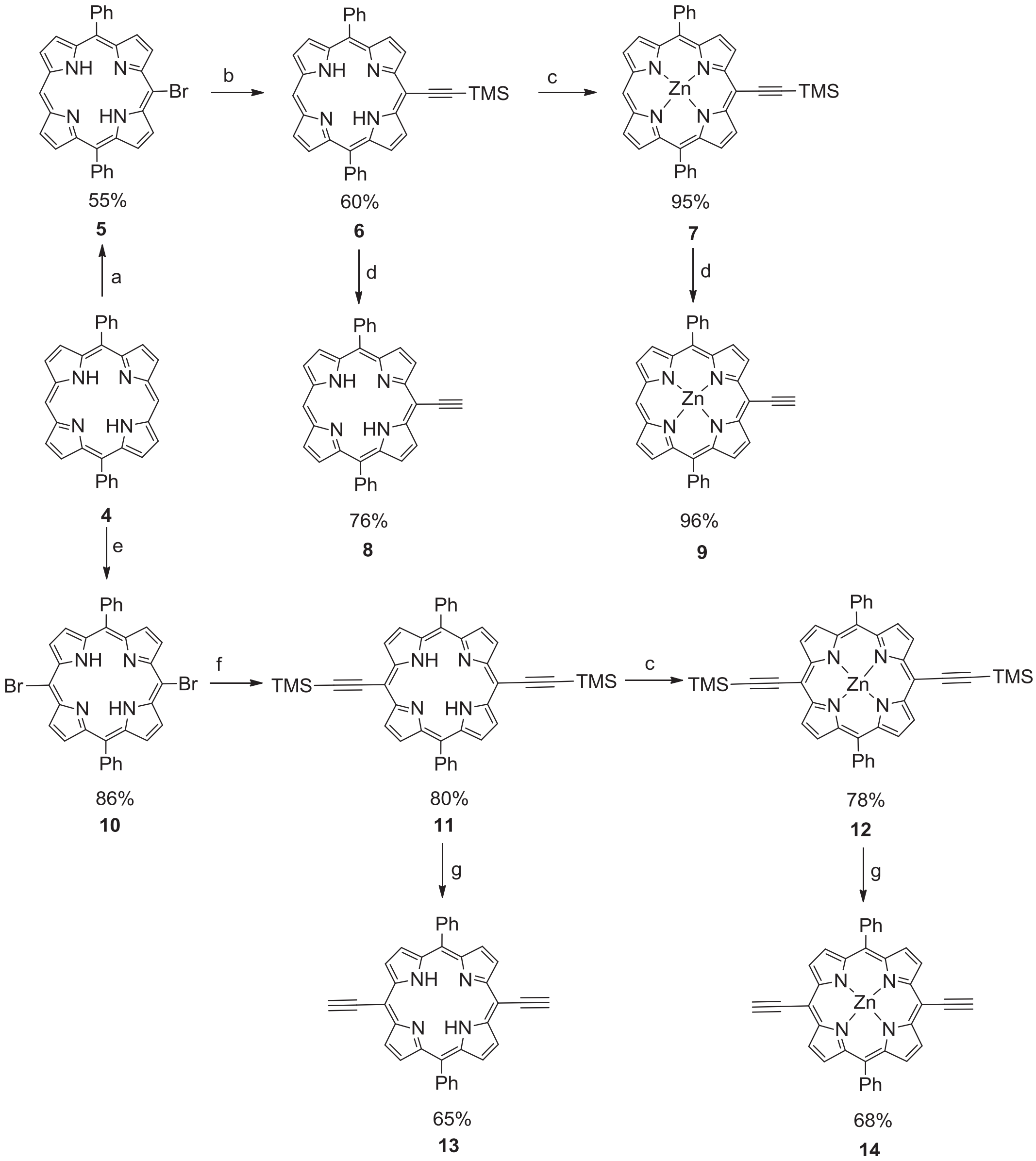

Scheme 2. Synthesis of 5-ethynyl- (**8** and **9**) and 5,15-diethynyl-substituted (**13** and **14**) porphyrins. Reagents and conditions: (a) NBS (1 equiv.), CH_2Cl_2/CH_3OH (9:1), rt, 15 min; (b) trimethylsilylacetylene (2 equiv.), $PdCl_2(Ph_3P)_2$, CuI, Et_3N/toluene; (c) $Zn(OAc)_2$, CH_3OH/toluene (1:4), reflux, 4 h; (d) TBAF (1.5 equiv.), CH_2Cl_2, rt, 30 min; (e) NBS (2.5 equiv.), pyridine, $CHCl_3$, 0 °C, 1 h; (f) trimethylsilylacetylene (4 equiv.), $PdCl_2(Ph_3P)_2$, CuI, Et_3N/toluene; (g) TBAF (2 equiv.), CH_2Cl_2, rt, 30 min.

dyad **15** belong to phenyl protons of the compound. The disappearance of the signal at 4.13 ppm corresponding to the ethynyl proton confirmed the structure (Fig. S10). The Zn-porphyrin-Cu(III)-corrole dyad **16** showed similar properties to dyad **15** and same type of signal shifts were observed (Figs. S23–S25).

While the dyads **15** and **16** are soluble in $CDCl_3$, the triads **17** and **18** are more soluble in *d*-THF. The ^1H NMR spectrum of the triad **18** (Fig. 3) shows symmetric two sets of β-proton resonances of the porphyrin sub-unit as doublets at 9.55 and 8.73 ppm. β-Proton resonances of the corrole sub-units appear with over-lapping signals with phenyl protons between 7.3 and 7.7 ppm. Significant changes in the ^1H NMR spectra of the dyads **15**, **16** and the triads **17**, **18**, compared to the corresponding monomers, indicate interactions of the porphyrin and the corrole units with each other in the synthesized conjugates.

The absorption spectra of the corrole **3**, the porphyrin monomers, the dyads, and the triads were recorded in $CHCl_3$ (Table 1). Fig. 4 shows the comparison of absorption spectra of the dyad **15**, the corrole **3** and the porphyrin **8**. Though the dyad **15** showed a similar Soret band with corrole monomer **3** at 412 nm, its Q bands have different peak maxima than corresponding monomers at 508, 539, 581, and 649 nm. Similarly, the dyad **15**, the Zn-porphyrin containing dyad **16** showed different Q bands to those of constituent macrocycles (Fig. S37) and only one absorption band was determined at 548 nm. As shown in Fig. 5 and Fig. S38, absorption spectra of the triads **17** and **18** are a linear combination of the spectra of the corresponding monomers and interactions between porphyrin and corrole sub-units are weak.

The emission properties of the dyads **15**, **16** and the triads **17**, **18** were studied by steady state fluorescence technique at room temperature in chloroform in order to understand their excited state dynamics. Fig. 6 and Fig. S39 show the emission spectra of the dyads **15** and **16**, their monomers and 1:1 mixtures of the corresponding monomers at λ = 420 nm. Cu(III)-corrole monomer **3** is

Please cite this article in press as: B. Temelli, et al., Ethynyl-bridged porphyrin-corrole dyads and triads: Synthesis, properties and DFT calculations, Tetrahedron (2018), https://doi.org/10.1016/j.tet.2018.07.007

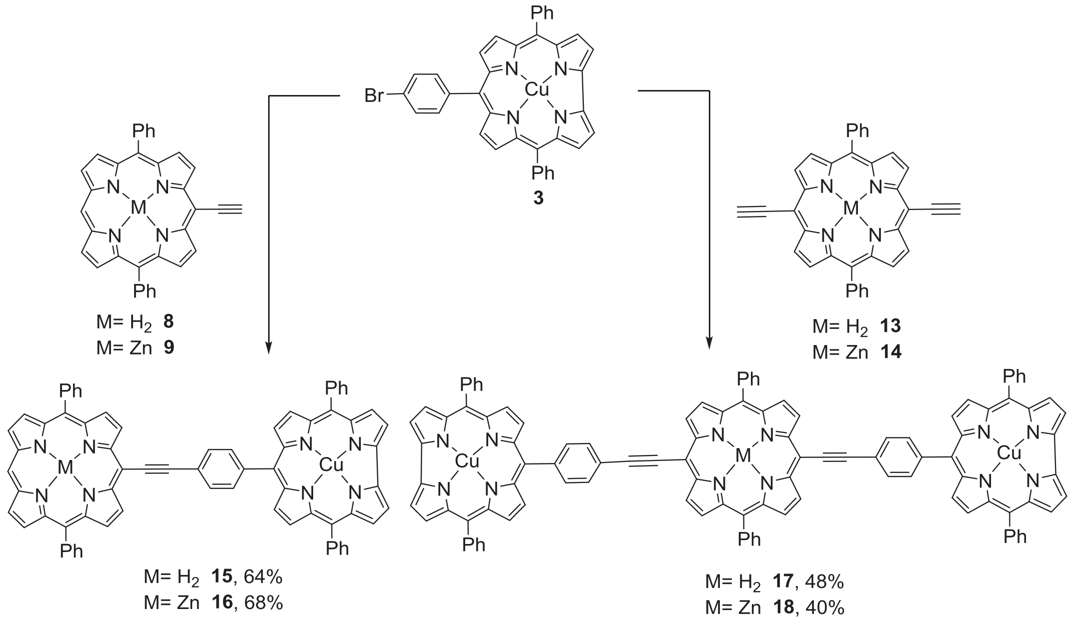

Scheme 3. Synthesis of dyads (**15** and **16**) and triads (**17** and **18**).

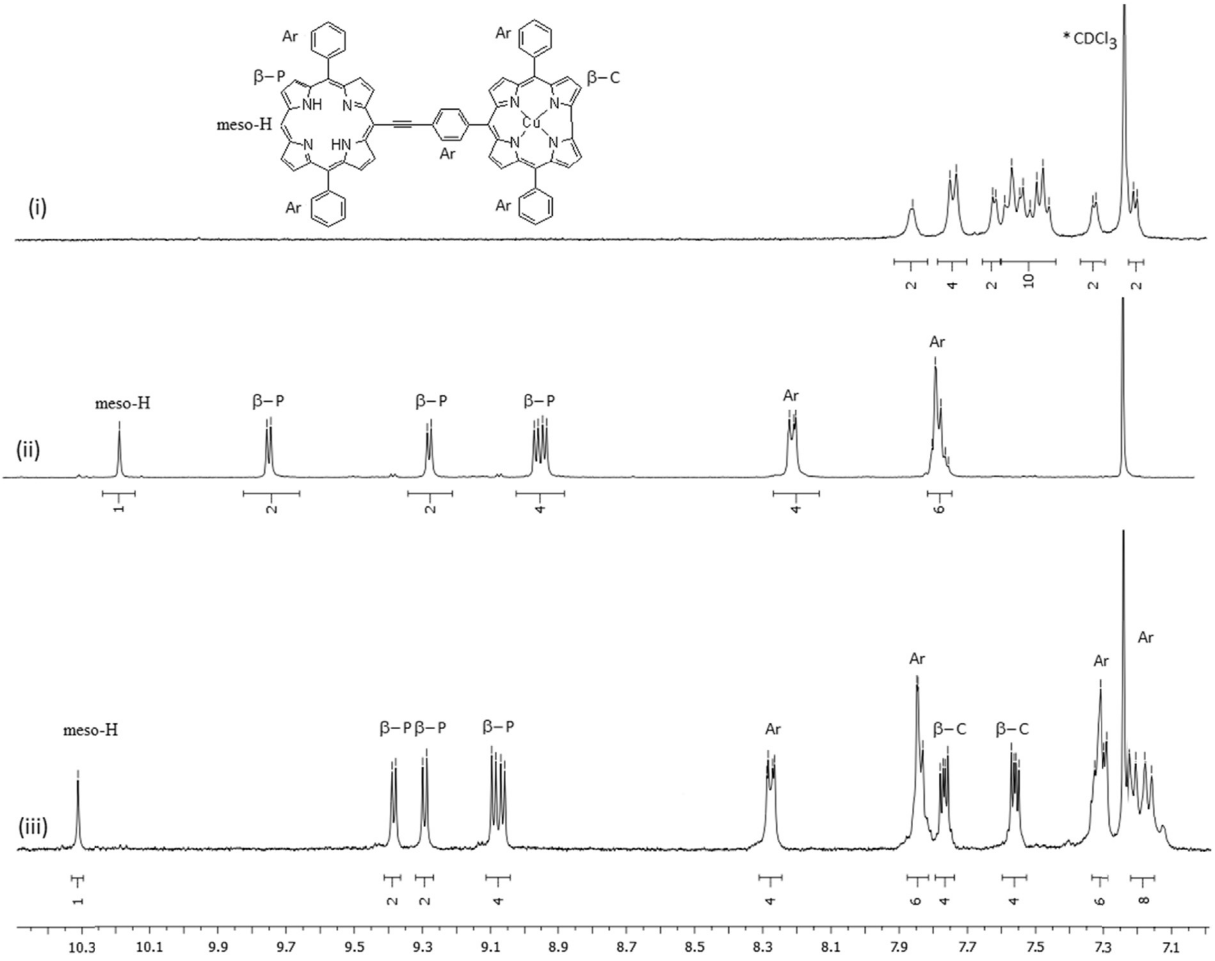

Fig. 2. Comparison of the ^{1}H NMR spectra of (i) corrole **3** (ii) porphyrin **8** and (iii) dyad **15**.

nonfluorescent and the porphyrin monomer **8** showed two emissions at 653 nm and 723 nm. The emission from the porphyrin monomer was quenched by 70% in dyad **15**. No significant quenching was observed when 1:1 mixture of the porphyrin **8** and corrole **3** was excited (Fig. 6). The emission spectrum of the dyad **16** showed emissions at 596 nm and 650 nm. The comparison of the emission spectra of the dyad **16** and the monomer **9** indicates that the emission from porphyrin unit decreased at 596 nm, while the

Please cite this article in press as: B. Temelli, et al., Ethynyl-bridged porphyrin-corrole dyads and triads: Synthesis, properties and DFT calculations, Tetrahedron (2018), https://doi.org/10.1016/j.tet.2018.07.007

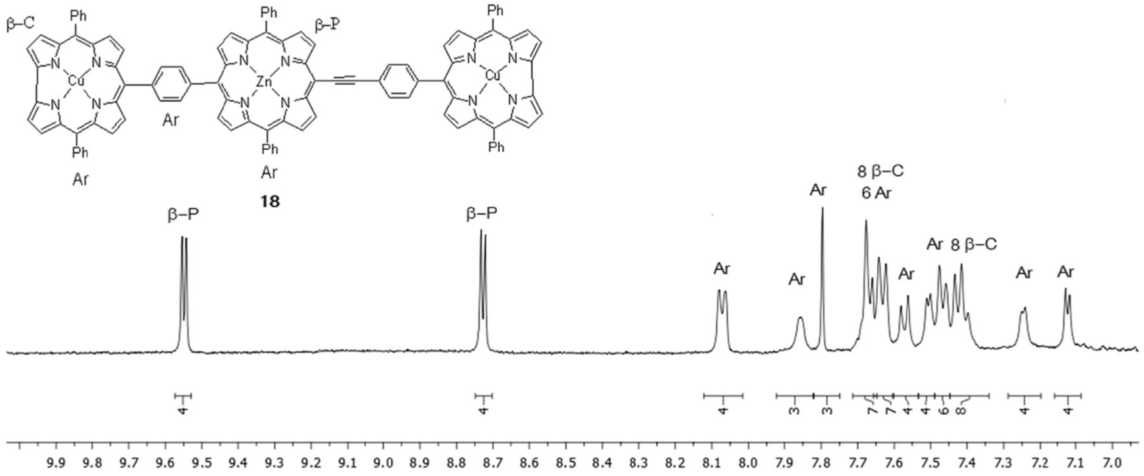

Fig. 3. The ^{1}H NMR spectra of triad **18**.

Table 1
Absorption data for dyads (**15, 16**) and triads (**17, 18**) and their corresponding monomers recorded in chloroform.

Comp.	Soret band λ [nm] (log ε)	Q bands	λ [nm] (log ε)		
3	412 (4.69)	528 (3.59)	603 (3.40)		
8	420 (5.50)	517 (4.20)	552 (3.90)	593 (3.68)	649 (3.34)
9	419 (5.01)	550 (3.68)	587 (3.33)		
13	427 (5.32)	531 (4.02)	571 (4.24)	608 (3.64)	670 (3.83)
14	430 (5.29)	575 (3.90)	622 (4.11)		
15	413 (4.13)	508 (3.14)	539 (2.62)	581 (2.68)	649 (1.84)
16	418 (4.47)	548 (3.36)			
17	427 (4.83)	532 (3.76)	571 (3.91)	609 (3.46)	670 (3.58)
18	441 (4.59)	531 (3.65)	575 (3.76)	622 (3.90)	

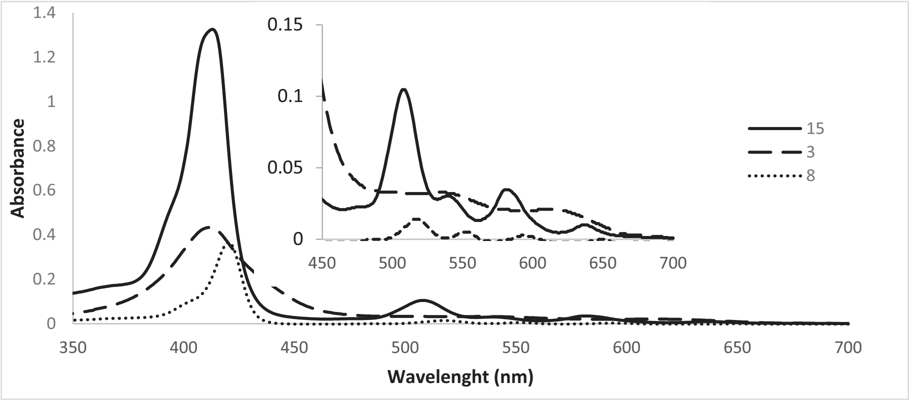

Fig. 4. Absorption spectra of dyad **15** and its monomers corrole **3** and porphyrin **8** in $CHCl_3$ (10^{-5} M).

emission at 650 nm increasing (Fig. S39).

Same type of quenching properties and energy transfer from the porphyrin to the corrole sub-unit was observed for the triads **17** and **18**. The comparison of fluorescence spectra of the triad **17** with its monomers shows that the emission from metal free-porphyrin unit was quenched by 95%. The same amount of emission was obtained when 1:1 mixture of the porphyrin **13** and corrole **3** compounds was excited (Fig. 7). Similarly, the emission from porphyrin-Zn complex was also quenched by 76% in triad **18** (Fig. S40). These results suggest that there is a significant intermolecular association between the sub-units and the energy transfer from the porphyrin to the corrole unit in the dyads and triads. Similar type of observations were noted in related porphyrin donor-corrole acceptor systems in the literature [4f,4g,13].

2.1. Computational results

Based on the structures given in Scheme 3 (**3**, **8**, **9**, **13**–**18**), nine model geometries were designed for the computational studies. All structures were optimized to their lowest energy geometries at B3LYP/6-311G(d,p) level of DFT.

Due to the noninnocence character of the corrole ligand, and the proposed equilibrium between singlet corrole-copper(III) and triplet corrole-copper(II) radical cation [14,15], geometry optimizations were performed according to three different spin states, which are closed shell singlet, triplet and open shell singlet states.

Please cite this article in press as: B. Temelli, et al., Ethynyl-bridged porphyrin-corrole dyads and triads: Synthesis, properties and DFT calculations, Tetrahedron (2018), https://doi.org/10.1016/j.tet.2018.07.007

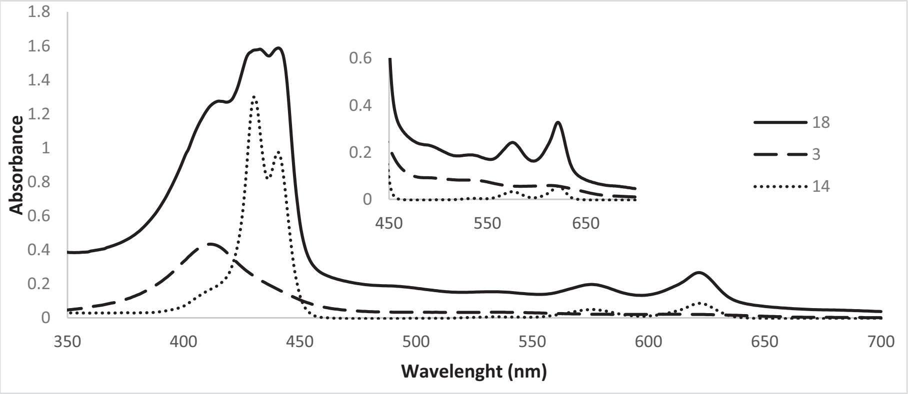

Fig. 5. Absorption spectra of triad **18** and its monomers corrole **3** and porphyrin **14** in $CHCl_3$ (10^{-5} M).

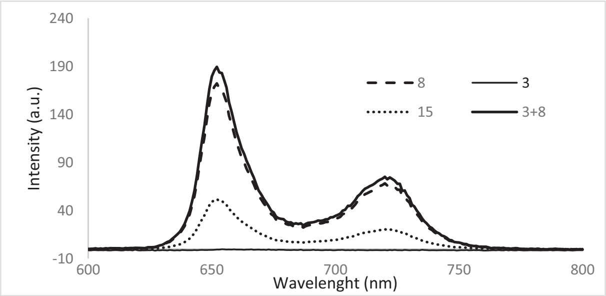

Fig. 6. Emission spectra of corrole **3**, porphyrin **8**, dyad **15** and the mixture of **3** and **8** at room temperature ($CHCl_3$, λ = 420 nm).

Open shell singlet state was found as the ground state for corrole-copper containing structures (**3**, **15**–**18**), which is more stable than the corresponding closed shell singlet state by 0.153, 0.156, 0.156, 0.313, and 0.314 eV for **3**, **15**, **16**, **17** and **18**, respectively (Figs. S41–S45). This result is also in agreement with previous experimental and computational studies suggesting an antiferromagnetically coupled Cu(II) corrole radical cation as the ground state for copper corrole [16–19]. For other structures (**8**, **9**, **13** and **14**) closed shell singlet state is the ground state.

Calculated bond lengths and bond angles of the corrole **3** and the porphyrin monomers **8**, **9**, **13** and **14** are found similar to their formerly reported analogs [10]. In the optimized geometries of both the dyads (**15** and **16**) and the triads (**17** and **18**), porphyrin moieties lie approximately on the same plane with the bridging phenyl groups, where corrole components lie in different planes. The angle between the least square planes of corrole and porphyrin moieties is 54.6 degrees for **15** and 53.9 degrees for **16**. In triads **17** and **18**, the angle between each corrole plane and the porphyrin plane is 50.6 and 50.8 degrees, respectively, and the angle between the two corrole planes are 102.3 degrees. More detailed data about the optimized geometries and the cartesian coordinates of the model structures are available in Supporting Information.

Calculated orbital energy levels from HOMO-5 to LUMO+5 for the model molecules are presented in Table 2 and Fig. 8. The energy gap (E_g) between the HOMO and the LUMO for corrole monomer **3** and porphyrin monomers **8**, **9**, **13** and **14** are 2.607(1.552), 2.631, 2.704, 2.457 and 2.527 eV, respectively. E_g α and β, in parentheses, for the corresponding dyads (**15**, **16**) and the triads (**17**, **18**) are 1.543 (2.115), 1.544 (2.180), 1.270 (1.270) and 1.270 (1.270), respectively. It is seen that the dyads and triads have considerably smaller E_g values than their corresponding porphyrin components. Especially orbital energy levels of the triads are very close to each other, and degenerated frontier molecular orbitals were observed.

To investigate charge separation and donor-acceptor properties between macrocycles of the dyads (**15** and **16**) and the triads (**17** and **18**), molecular models shown in Fig. 9 a and b were used.

The electron density distributions and corresponding energies for the selected molecular orbitals of **15**–**18** are shown in Figs. 10 and 11 (See also S46–S49). Related molecular orbital compositions calculated at B3LYP/6-311G(d,p) level are given in Tables 3 and 4.

In the dyads **15** and **16**, the HOMOα, HOMOβ and the LUMOα molecular orbitals are located on the corrole moiety, whereas the LUMOβ molecular orbital locates on the porphyrin moiety in great extent (Fig. 10 and Table 3). Calculated electronic spectra (Table 5)

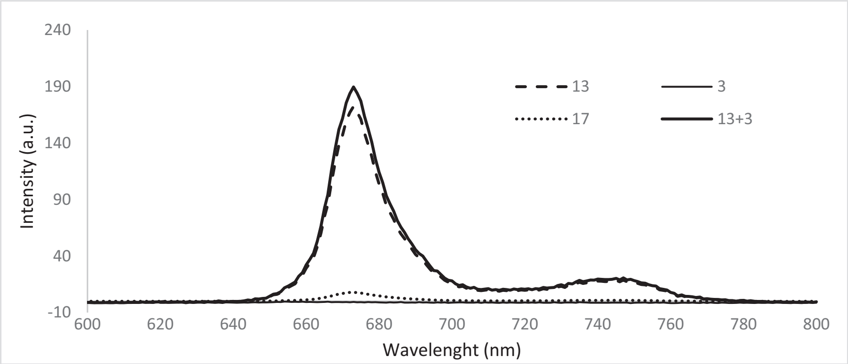

Fig. 7. Emission spectra of corrole **3**, porphyrin **13**, triad **17** and the mixture of **3** and **13** at room temperature ($CHCl_3$, λ = 420 nm).

Please cite this article in press as: B. Temelli, et al., Ethynyl-bridged porphyrin-corrole dyads and triads: Synthesis, properties and DFT calculations, Tetrahedron (2018), https://doi.org/10.1016/j.tet.2018.07.007

Table 2
Selected orbital energies (eV) calculated at B3LYP/6-311G(d,p) level.

	3α	**3β**	**8**	**9**	**13**	**14**	**15α**	**15β**	**16α**	**16β**	**17α,β**	**18α,β**
LUMO+5	−0.520	−0.500	−0.452	−0.420	−0.485	−0.455	−1.186	−1.224	−1.130	−1.168	−2.039	−2.031
LUMO+4	−0.770	−0.736	−0.485	−0.448	−0.524	−0.487	−1.700	−1.672	−1.684	−1.663	−2.051	−2.038
LUMO+3	−0.781	−0.762	−0.494	−0.454	−0.527	−0.491	−2.017	−1.999	−2.008	−1.985	−2.330	−2.324
LUMO+2	−1.751	−1.749	−1.052	−0.964	−1.226	−1.151	−2.557	−2.310	−2.460	−2.301	−2.601	−2.522
LUMO+1	−2.082	−2.091	−2.546	−2.438	−2.589	−2.497	−2.752	−2.561	−2.674	−2.464	−2.979	−2.906
LUMO	−2.384	−3.669	−2.679	−2.590	−2.881	−2.791	−3.600	−2.762	−3.589	−2.684	−3.630	−3.620
[a]HOMO	−4.991	−5.221	−5.310	−5.294	−5.338	−5.317	−5.142	−4.877	−5.133	−4.865	−4.899	−4.890
[a]HOMO-1	−5.193	−5.596	−5.581	−5.480	−5.650	−5.554	−5.231	−5.114	−5.214	−5.104	−5.138	−5.130
[a]HOMO-2	−6.533	−6.486	−6.584	−6.771	−6.609	−6.720	−5.525	−5.262	−5.507	−5.246	−5.167	−5.159
[a]HOMO-3	−6.631	−6.573	−6.701	−6.798	−6.745	−6.851	−5.601	−5.604	−5.516	−5.510	−5.218	−5.207
[a]HOMO-4	−6.781	−6.715	−6.985	−6.798	−6.989	−6.888	−6.412	−6.453	−6.403	−6.446	−5.548	−5.540
[a]HOMO-5	−6.834	−6.808	−7.067	−6.831	−7.096	−6.892	−6.416	−6.458	−6.406	−6.449	−5.675	−5.588
E_g	**2.607**	**1.552**	**2.631**	**2.704**	**2.457**	**2.527**	**1.543**	**2.115**	**1.544**	**2.180**	**1.270**	**1.270**

[a] For structures at their open shell singlet states (**3**, **15**–**18)** singly occupied.

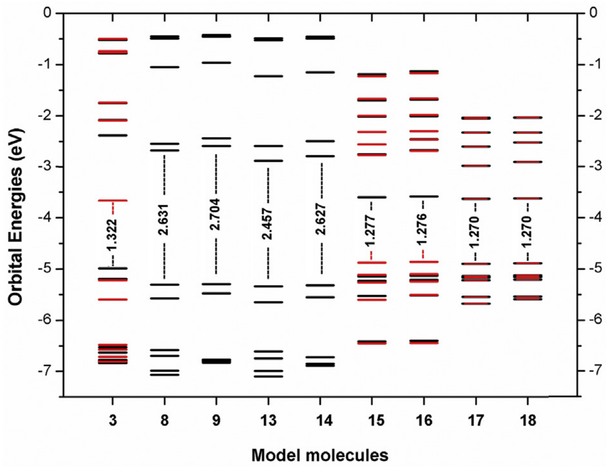

Fig. 8. Orbital energy levels (from HOMO-5 to LUMO+5) calculated at B3LYP/6-311G(d,p) level (red lines represent β molecular orbitals for the structures at open shell singlet state). (For interpretation of the references to colour in this figure legend,

indicates that the lowest energy UV–vis transition in the dyads was between the HOMOβ and the LUMOβ, and charge separation between these two orbitals has been observed. In the triads **17** and **18**, again the HOMO and the LUMO are located greatly on the corrole moieties (Fig. 11 and Table 4), and charge separation has been achieved via transition between the HOMO and the LUMO+1 orbitals.

3. Conclusions

The first synthesis of ethynyl-bridged porphyrin-corrole dyads and triads was achieved by using Sonogashira coupling reactions. The absorption and emission spectra indicate that the emission of porphyrin unit in the dyads and the triads were quenched significantly by corrole unit. On the basis of the DFT calculations, geometric and electronic properties of the new molecules have been discussed. Charge separated donor-acceptor property between porphyrin and corrole moieties has been observed for the dyads and the triads.

4. Experimental section

4.1. General

All solvents and reagents were obtained from Aldrich Chemicals and Acros Organics. NMR spectra were recorded by using Bruker DPX-400 Ultra Shield spectrometer and chemical shifts are reported in parts per million (ppm) relative to TMS. Mass spectra were recorded with Agilent 6224 TOF LC-MS instrument. Infrared spectra were measured by using a Thermo Scientific, Nicolet IS10 spectrometer. Absorption spectra were obtained with PG T80. Fluorescence spectra were recorded with Varian Cary Eclipse spectrometer. Flash column chromatography was performed on Silica (Merck, Kiesegel, 230–400 mesh). 2,2'-(Phenylmethylene) bis(1*H*-pyrrole) (**1**) [20], 5,15-diphenylporphyrin (**4**) [21], 5-bromo-10,20-diphenylporphyrin (**5**) [22], and 5,15-dibromo-10,20-diphenylporphyrin (**10**) [15] were synthesized by the reported methods.

4.2. 10-(4-Bromophenyl)-5,15-diphenylcorrole (2)

2,2'-(Phenylmethylene)bis(1*H*-pyrrole) (**1**) (1.00 g, 4.50 mmol) and *p*-bromobenzaldehyde (0.42 g, 2.25 mmol) were dissolved in CH_3OH (225 mL) and a HCl solution (36%, 11.25 mL) in H_2O (225 mL) was added to the reaction mixture at room temperature. After 1 h, the aqueous phase was extracted with $CHCl_3$ (3 × 100 mL) and diluted to 750 mL. *p*-Chloranil (1.66 g, 6.75 mmol) was added and the reaction mixture was stirred 24 h. The solvent was removed

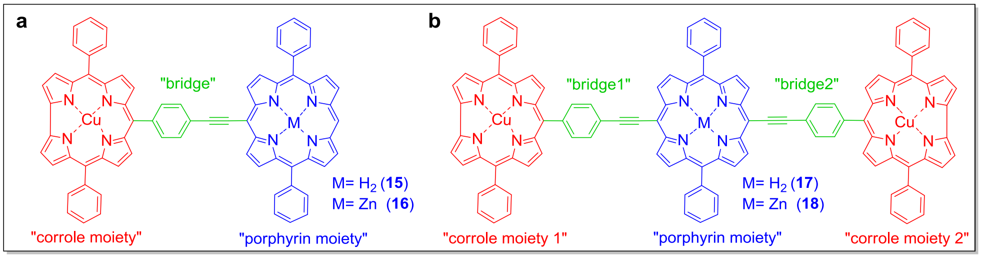

Fig. 9. Model structures for dyads (a) and triads (b).

Please cite this article in press as: B. Temelli, et al., Ethynyl-bridged porphyrin-corrole dyads and triads: Synthesis, properties and DFT calculations, Tetrahedron (2018), https://doi.org/10.1016/j.tet.2018.07.007

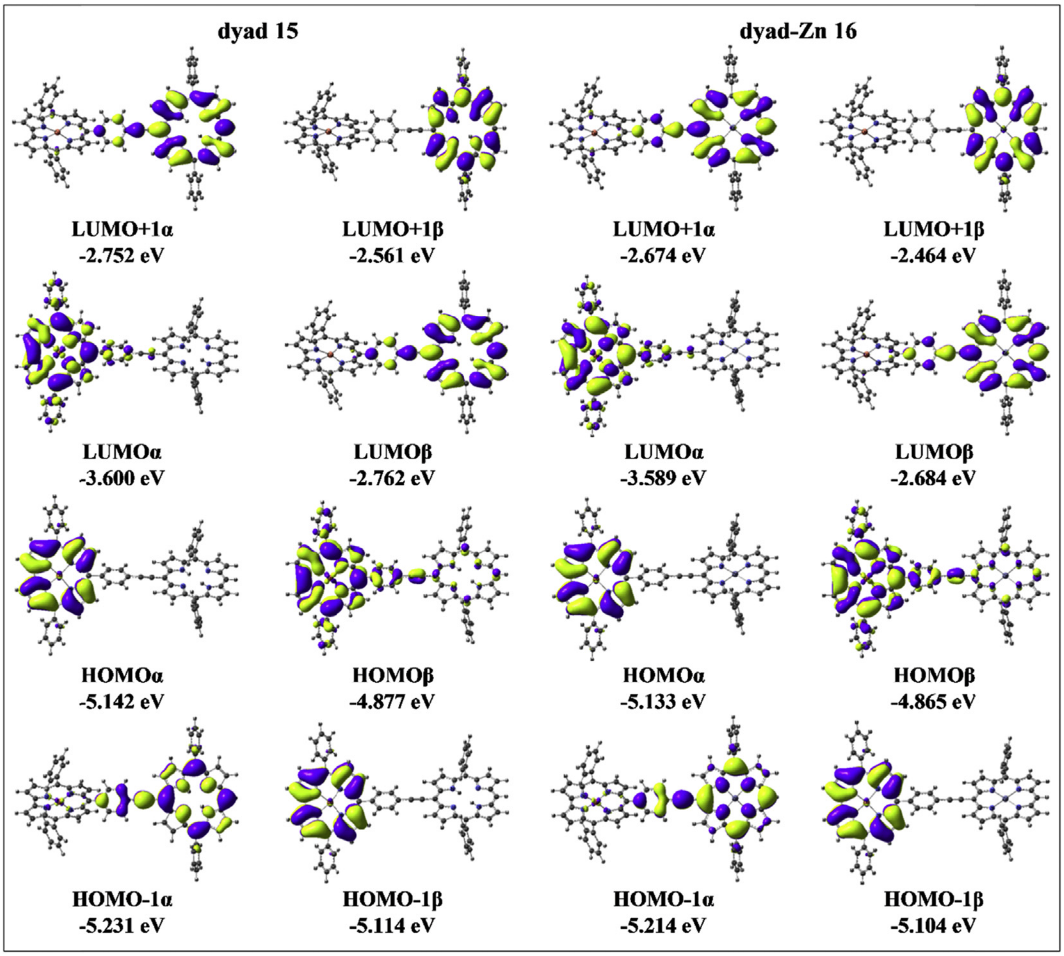

Fig. 10. Selected FMOs of the dyads **15** and **16**.

under reduced pressure. The crude product was purified by flash column chromatography (CH_2Cl_2/hexanes 1:6) to provide **2** (463 mg, 34%) as a green solid: m.p.> 300 °C; R_f: 0.55 (EtOAc/hexanes 1:10); IR (ATR, cm^{-1}) ν 3393, 3345, 1803, 1754, 1687, 1550, 1480, 1461, 1437, 1413, 1381, 1333, 1309, 1283, 1239, 1225, 1212, 1174, 1109, 1069, 1033, 1010, 961, 922, 909, 874, 845, 820, 785, 756, 717, 700, 663; UV/Vis ($CHCl_3$) λ_{max} (log ε): 416 (4.49), 575 (3.61), 614 (3.50), 647 3.43) nm; ^1H NMR (400 MHz, $CDCl_3$) δ 8.85 (br s, 4H), 8.51 (br s, 4H), 8.33 (d, $J = 6.8$ Hz, 4H, Ph-H), 8.01 (d, $J = 7.5$ Hz, 2H, Ph-H), 7.91–7.69 (m, 8H); ^{13}C NMR (100 MHz, $CDCl_3$) δ 143.2, 136.3, 135.2, 132.4, 131.8, 130.8, 130.7, 130.6, 128.9–127.5 (overlapping peaks), 118.9, 108.2; HRMS (ESI): *m/z* calcd for $C_{37}H_{26}BrN_4$ $[M+H]^+$ 605.1335, found 605.1348.

4.3. 10-(4-Bromophenyl)-5,15-diphenylcorrole-copper(III) (*3*)

10-(4-Bromophenyl)-5,15-diphenylcorrole (**2**) (0.200 g, 0.330 mmol) and $Cu(OAc)_2.H_2O$ (0.200 g, 0.990 mmol) were dissolved in THF (45 mL) and the reaction mixture was stirred at room temperature for 30 min. The solvent was removed under reduced pressure and the product was purified by flash column chromatography ($CHCl_3$) to provide **3** (196 mg, 89%) as a green solid: m.p.> 300 °C; R_f: 0.62 (EtOAc/hexanes 1:10); IR (ATR, cm^{-1}) ν 3358, 1678, 1565, 1517, 1491, 1466, 409, 1365, 1338, 1309, 1251, 1191, 1108, 1070, 1052, 1020, 1009, 982, 881, 843, 811, 789, 768, 756, 731, 706, 675, 661; UV/Vis ($CHCl_3$) λ_{max} (log ε): 412 (4.69), 528 (3.59), 603 (3.40) nm; ^1H NMR (400 MHz, $CDCl_3$) δ 7.80 (br s, 2H, β-H), 7.67 (d, $J = 7.2$ Hz, 4H, Ph-H), 7.55 (d, $J = 3.7$ Hz, 2H, β-H), 7.53–7.38 (m, 10H, Ph-H), 7.26 (d, $J = 4.0$ Hz, 2H, β-H), 7.14 (d, $J = 4.3$ Hz, 2H, β-H); HRMS (ESI): *m/z* calcd for $C_{37}H_{23}BrCuN_4$ $[M+H]^+$ 665.0397, found 665.0348.

4.4. 5-Trimethylsilylethynyl-10,20-diphenylporphyrin (*6*)

A solution of 5-bromo-10,20-diphenylporphyrin (**5**) (0.300 g, 0.554 mmol), trimethylsilylacetylene (15 μL, 1.11 mmol), $PdCl_2(Ph_3P)_2$ (11.4 mg, 0.0161 mmol), and copper(I) iodide (3.35 mg, 0.0177 mmol) in Et_3N/toluene (2:1, 50 mL) was deoxygenated and stirred at 80 °C under N_2 atmosphere. After 6 h, the mixture was cooled to room temperature and filtered. The solvent was removed under reduced pressure. The crude product was purified by flash column chromatography ($CHCl_3$:hexanes 1:2) to provide **6** (162 mg, 60%) as a purple solid: m.p.> 300 °C; R_f: 0.70 (EtOAc/hexanes 1:6); IR (ATR, cm^{-1}) ν 2955, 2919, 2850, 2138, 1737, 1597, 1556, 1456, 1440, 1404, 1341, 1245, 1197, 1181, 1153, 1118, 1064, 1051, 1031, 1001, 991, 957, 839, 749, 739, 724, 702, 690, 655; UV/Vis ($CHCl_3$) λ_{max} (log ε): 424 (5.25), 522 (3.93), 558 (3.86), 595 (3.50), 653 (3.34) nm; ^1H NMR (400 MHz, $CDCl_3$) δ 9.93 (s, 1H, meso-H), 9.65 (d, $J = 4.7$ Hz, 2H, β-H), 9.06 (br s, 2H, β-H), 8.84 (d, $J = 4.6$ Hz, 2H, β-H), 8.78 (d, $J = 3.6$ Hz, 2H, β-H), 8.10–8.06 (m, 4H, Ph-H), 7.66–7.63 (m, 6H, Ph-H), 0.52 (s, 9H, CH_3), −2.81 (s, 2H, NH); ^{13}C NMR (100 MHz, $CDCl_3$) δ 140.9, 134.3, 131.2, 130.8, 130.5, 127.5, 126.5, 120.1, 107.1, 106.2, 101.5, 99.1, 0.00; HRMS (ESI): *m/z* calcd for $C_{37}H_{31}N_4Si$ $[M+H]^+$ 559.2312, found 559.2323.

Please cite this article in press as: B. Temelli, et al., Ethynyl-bridged porphyrin-corrole dyads and triads: Synthesis, properties and DFT calculations, Tetrahedron (2018), https://doi.org/10.1016/j.tet.2018.07.007

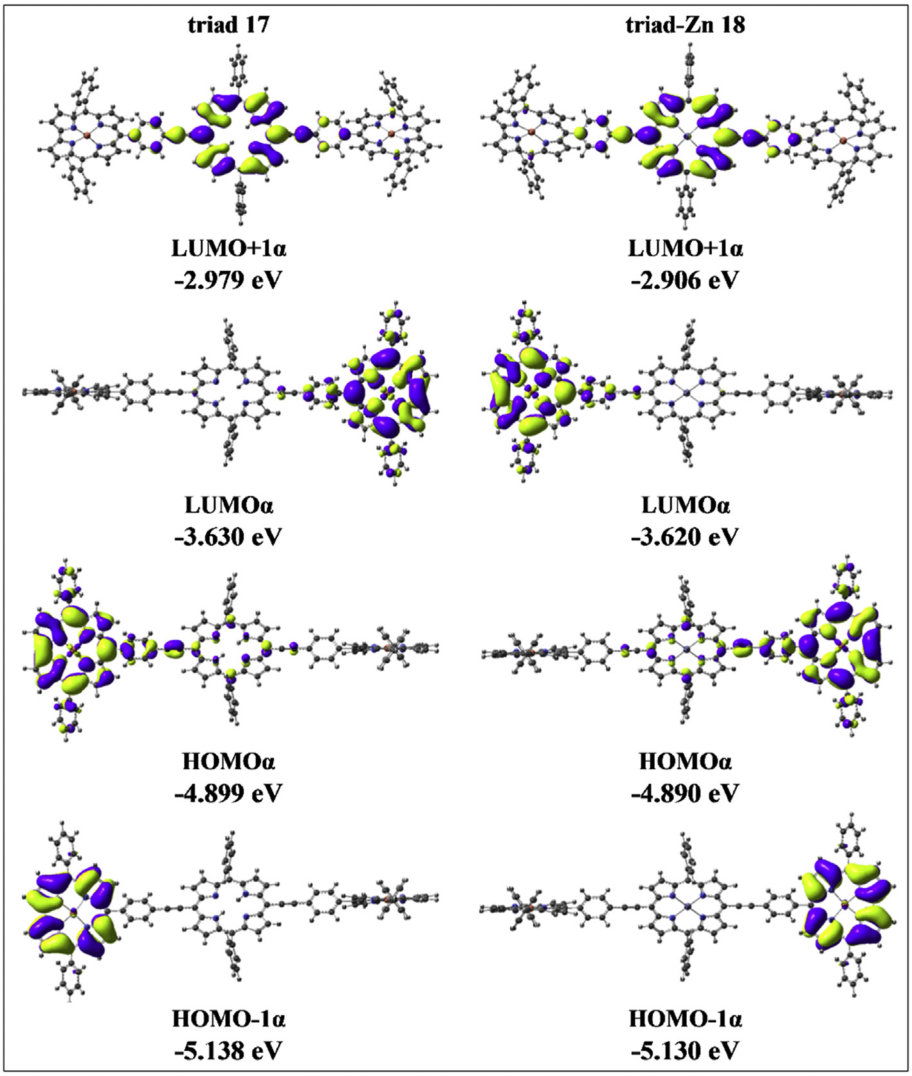

Fig. 11. Selected FMOs of the triads.

Table 3
Energies and percent compositions of selected frontier molecular orbitals of dyads.

Species	α MO	Energy (eV)	% compositions			β MO	Energy (eV)	% compositions		
			C	B	P			C	B	P
dyad **15**	L+2	−2.557	0	0	100	L+2	−2.310	99	1	0
	L+1	−2.752	3	12	85	L+1	−2.561	0	0	100
	L	−3.600	94	5	2	L	−2.762	2	13	85
	H	−5.142	100	0	0	H	−4.877	86	7	7
	H-1	−5.231	3	19	78	H-1	−5.114	99	1	0
	H-2	−5.525	98	0	1	H-2	−5.262	10	16	73
dyad **16**	L+2	−2.460	0	0	100	L+2	−2.301	99	1	0
	L+1	−2.674	3	13	84	L+1	−2.464	0	0	100
	L	−3.589	94	5	2	L	−2.684	3	14	84
	H	−5.133	100	0	0	H	−4.865	85	8	7
	H-1	−5.214	3	20	77	H-1	−5.104	99	1	0
	H-2	−5.507	0	0	100	H-2	−5.246	11	17	72

H: highest energy singly occupied molecular orbital, L: lowest energy unoccupied molecular orbital, P: porphyrin moiety C: corrole moiety B: bridge.

*4.5. 5-Trimethylsilylethynyl-10,20-diphenylporphyrinato-zinc(II) (**7**)*

5-Trimethylsilylethynyl-10,20-diphenylporphyrin (**6**) (0.100 g, 0.18 mmol) and $Zn(OAc)_2.2H_2O$ (0.138 g, 0.63 mmol) were dissolved in a mixture of CH_3OH (6 mL) and toluene (22 mL). The mixture was refluxed for 4 h. in the dark and cooled to room temperature. The solvent was removed under reduced pressure. The crude product was washed with hot water and dried to provide **7** (106 mg, 95%) as a purple solid: m.p.> 300 °C; R_f: 0.85 (EtOAc/hexanes 1:3); IR (ATR,

Please cite this article in press as: B. Temelli, et al., Ethynyl-bridged porphyrin-corrole dyads and triads: Synthesis, properties and DFT calculations, Tetrahedron (2018), https://doi.org/10.1016/j.tet.2018.07.007

Table 4
Energies and percent compositions of selected frontier molecular orbitals of triads.

Species	α MO	Energy (eV)	% compositions					β MO	Energy (eV)	% compositions				
			C1	B1	P	B2	C2			C1	B1	P	B2	C2
triad **17**	L+2	−2.601	0	0	100	0	0	L+2	−2.601	0	0	100	0	0
	L+1	−2.979	2	11	75	10	3	L+1	−2.979	3	10	75	11	2
	L	−3.630	0	0	2	5	93	L	−3.630	93	5	2	0	0
	H	−4.899	84	7	7	1	0	H	−4.899	0	1	7	7	84
	H-1	−5.138	100	0	0	0	0	H-1	−5.138	0	0	0	0	100
	H-2	−5.167	0	0	0	0	100	H-2	−5.167	100	0	0	0	0
triad **18**	L+2	−2.522	0	0	100	0	0	L+2	−2.522	0	0	100	0	0
	L+1	−2.906	3	10	74	11	2	L+1	−2.906	2	11	74	10	3
	L	−3.620	93	5	2	0	0	L	−3.620	0	0	2	5	93
	H	−4.890	0	1	8	8	83	H	−4.890	83	8	8	1	0
	H-1	−5.130	0	0	0	0	100	H-1	−5.130	100	0	0	0	0
	H-2	−5.159	100	0	0	0	0	H-2	−5.159	0	0	0	0	100

H: highest energy singly occupied molecular orbital, L: lowest energy unoccupied molecular orbital, P: porphyrin moiety C: corrole moiety B: bridge.

Table 5
Calculated lowest energy UV–vis electronic transition data for dyads and triads.

Species	E_g/eV	λ_{max}/nm(eV)	*f*	Major Contributions	Transition[a]
dyad **15**	1.277	665 (1.864)	0.1744	HOMOβ → LUMOβ (64%)	C→P
dyad **16**	1.276	651 (1.904)	0.1841	HOMOβ → LUMOβ (60%)	C→P
triad **17**	1.270	745 (1.665)	0.5997	HOMO →LUMO+1 (47%)	C→P
triad **18**	1.270	722 (1.717)	0.6192	HOMO →LUMO+1 (45%)	C→P

[a] P: porphyrin moiety C: corrole moiety.

cm^{-1}) ν 3110, 3059, 2962, 2907, 2853, 2118, 2102, 1806, 1593, 1488, 1440, 1379, 1314, 1247, 1213, 1155, 1064, 1004, 994, 835, 785, 749, 731, 696, 667, 657; UV/Vis ($CHCl_3$) λ_{max} (log ε): 424 (5.57), 554 (4.21), 592 (3.85) nm; ^1H NMR (400 MHz, $CDCl_3$) δ 10.08 (s, 1H, meso-H), 9.72 (d, *J* = 4.6 Hz, 2H, β-H), 9.23 (d, *J* = 4.5 Hz, 2H, β-H), 8.95 (d, *J* = 4.6 Hz, 2H, β-H), 8.93 (d, *J* = 4.4 Hz, 2H, β-H), 8.17–8.11 (m, 4H, Ph-H), 7.76–7.69 (m, 6H, Ph-H), 0.54 (s, 9H, CH_3); ^{13}C NMR (100 MHz, $CDCl_3$) δ 151.7, 149.9, 149.4, 148.8, 141.9, 134.1, 132.4, 131.9, 131.4, 130.6, 127.1, 126.2, 120.9, 107.3, 106.9, 100.9, 99.5, 0.01; HRMS (ESI): *m/z* calcd for $C_{37}H_{29}N_4SiZn$ $[M+H]^+$ 621.1447, found 621.1435.

4.6. 5-Ethynyl-10,20-diphenylporphyrin (*8*)

5-Trimethylsilylethynyl-10,20-diphenylporphyrin (**6**) (0.070 g, 0.125 mmol) was dissolved in 4 mL of CH_2Cl_2 and TBAF (0.188 mL 0.188 mmol) was added to the solution. After 30 min, CH_3CO_2H (21 μL) and CH_3OH (7 mL) were added to the reaction. The mixture was filtered after 30 min and the solid product was washed with methanol to provide **8** (46 mg,76%) as a purple solid: m.p.> 300 °C; R_f: 0.79 (EtOAc/hexanes 1:3); IR (ATR, cm^{-1}) ν 3274, 3053, 2091, 1809, 1596, 1551, 1481, 1436, 1402, 1341, 1250, 1196, 1178, 1156, 1071, 1056, 959, 917, 859, 789, 726, 698; UV/Vis ($CHCl_3$) λ_{max} (log ε): 420 (5.50), 517 (4.20), 552 (3.90), 593 (3.68), 649 (3.34) nm; ^1H NMR (400 MHz, $CDCl_3$) δ 10.13 (s, 1H, meso-H), 9.69 (d, *J* = 4.5 Hz, 2H, β-H), 9.22 (d, *J* = 4.5 Hz, 2H, β-H), 8.90 (d, *J* = 4.7 Hz, 2H, β-H), 8.88 (d, *J* = 4.0 Hz, 2H, β-H), 8.17–8.13 (m, 4H, Ph-H), 7.77–7.68 (m, 6H, Ph-H), 4.13 (s, 1H, C≡CH), −2.80 (br s, 2H, NH); ^{13}C NMR (100 MHz, $CDCl_3$) δ 141.3, 134.7, 131.8, 131.7, 131.3, 130.8, 127.9, 127.0, 120.5, 106.8, 85.9, 84.0; HRMS (ESI): *m/z* calcd for $C_{34}H_{23}N_4$ $[M+H]^+$ 487.1917, found 487.1932.

4.7. 5-Ethynyl-10,20-diphenylporphyrinato-zinc(II) (*9*)

5-Trimethylsilylethynyl-10,20-diphenylporphyrinato-zinc(II) (**7**) (0.074 mg, 0.120 mmol) was dissolved in 4 mL of CH_2Cl_2 and TBAF (0.180 mL, 0.180 mmol) was added to the solution. After 30 min, CH_3CO_2H (21 μL) and CH_3OH (7 mL) were added to the reaction. The solvent was removed under reduced pressure and the crude product was purified by flash column chromatography (EtOAc/hexanes 1:3) to provide **9** (63 mg, 96%) as a purple solid: m.p.> 300 °C; R_f: 0.71 (EtOAc/hexanes 1:1); IR (ATR, cm^{-1}) ν 3260, 2918, 2849, 2069, 1800, 1724, 1595, 1523, 1487, 1462, 1440, 1379, 1314, 1258, 1212, 1173, 1155, 1123, 1066, 993, 935, 917, 908, 867, 823, 785, 744, 733, 715, 697, 672, 656; UV/Vis ($CHCl_3$) λ_{max} (log ε): 419 (5.01), 550 (3.68), 587 (3.33) nm; ^1H NMR (400 MHz, d_8-THF) δ 10.05 (s, 1H, meso-H), 9.61 (d, *J* = 4.6 Hz, 2H, β-H), 9.18 (d, *J* = 4.4 Hz, 2H, β-H), 8.82 (d, *J* = 4.5 Hz, 2H, β-H), 8.78 (d, *J* = 4.4 Hz, 2H, β-H), 8.09–8.05 (m, 4H, Ph-H), 7.65–7.62 (m, 6H, Ph-H), 4.45 (s, 1H, C≡CH); ^{13}C NMR (100 MHz, d_8-THF) δ 151.7, 150.0, 149.2 (two peaks), 142.6, 134.1, 132.3, 131.7, 131.3, 131.2, 130.2, 129.9, 128.2, 126.8, 125.9, 123.9, 120.4, 106.8, 97.6, 86.2, 83.1; HRMS (ESI): *m/z* calcd for $C_{34}H_{21}N_4Zn$ $[M+H]^+$ 549.1052, found 549.1048.

4.8. 5,15-Bis(trimethylsilylethynyl)-10,20-diphenylporphyrin (*11*)

A solution of 5,15-dibromo-10,20-diphenylporphyrin (**10**) (0.750 g, 1.21 mmol), trimethylsilylacethylene (0.522 g, 5.32 mmol), $PdCl_2(Ph_3P)_2$ (0.085 g, 0.121 mmol) and copper(I) iodide (0.025 g, 0.133 mmol) in Et_3N/toluene (3:1, 100 mL) was deoxygenated and stirred at 80 °C under N_2 atmosphere. After 7 h, the mixture was cooled to room temperature and filtered. The solvent was removed under reduced pressure. The crude product was purified by flash column chromatography (EtOAc/hexanes 1:10) to provide **11** (634 mg, 80%) as a green solid: m.p.> 300 °C; R_f: 0.67 (EtOAc/hexanes 1:10); IR (ATR, cm^{-1}) ν 3320, 3065, 2955, 2358, 2140, 1739, 1557, 1470, 1441, 1397, 1345, 1246, 1196, 1137, 1064, 1050, 972, 836, 794, 759, 746, 720, 699, 688, 660; UV/Vis ($CHCl_3$) λ_{max} (log ε): 432 (5.50), 542 (4.06), 582 (4.62), 618 (3.73), 678 (4.20) nm; ^1H NMR (400 MHz, $CDCl_3$) δ 9.54 (d, *J* = 4.7 Hz, 4H, β-H), 8.75 (d, *J* = 4.7 Hz, 4H, β-H), 8.10 (d, *J* = 7.3 Hz, 4H, Ph-H), 7.74–7.67 (m, 6H, Ph-H), 0.54 (s, 18 H, CH_3), −2.29 (br s, 2H, NH); ^{13}C NMR (100 MHz, $CDCl_3$) δ 141.3, 134.5, 128.0, 126.9, 121.8, 106.8, 102.7, 100.8, 0.00; HRMS (ESI): *m/z* calcd for $C_{42}H_{39}N_4Si_2$ $[M+H]^+$ 655.2708, found 655.2708.

Please cite this article in press as: B. Temelli, et al., Ethynyl-bridged porphyrin-corrole dyads and triads: Synthesis, properties and DFT calculations, Tetrahedron (2018), https://doi.org/10.1016/j.tet.2018.07.007

*4.9. 5,15-Bis(trimethylsilylethynyl)-10,20-diphenylporphyrinato-zinc(II) (**12**)*

5,15-Bis(trimethylsilylethynyl)-10,20-diphenylporphyrin (**11**) (0.070 g, 0.107 mmol) and $Zn(OAc)_2.2H_2O$ (0.219 g, 0.374 mmol) were dissolved in a mixture of CH_3OH (3 mL) and toluene (11 mL). The mixture was refluxed for 4 h. in the dark and cooled to room temperature. The crude product was washed with hot water and purified by flash column chromatography (EtOAc/hexanes 1:20) to provide **12** (60 mg, 78%) as a purple solid: m.p.> 300 °C; R_f: 0.87 (EtOAc/hexanes 1:6); IR (ATR, cm^{-1}) ν 2954, 2927, 2855, 2129, 2104, 1738, 1596, 1504, 1456, 1442, 1377, 1342, 1308, 1245, 1211, 1176, 1162, 1064, 1004, 993, 838, 792, 755, 737, 705, 664, 654; UV/Vis ($CHCl_3$) λ_{max} (log ε): 434 (5.51), 573 (4.07), 618 (4.40) nm; ^1H NMR (400 MHz, $CDCl_3$) δ 9.56 (d, *J* = 4.6 Hz, 4H, β-H), 8.78 (d, *J* = 4.4 Hz, 4H, β-H), 8.05 (d, *J* = 7.0 Hz, 4H, Ph-H), 7.70–7.60 (m, 6H, Ph-H), 0.48 (s, 18 H, CH_3); ^{13}C NMR (100 MHz, $CDCl_3$) δ 156.7, 153.2, 152.2, 150.2, 142.1, 138.0, 134.4, 132.8, 131.3, 127.7, 126.7; HRMS (ESI): *m/z* calcd for $C_{42}H_{37}N_4Si_2Zn$ $[M+H]^+$ 717.1843, found 717.1826.

*4.10. 5,15-Diethynyl-10,20-diphenylporphyrin (**13**)*

5,15-Bis(trimethylsilylethynyl)-10,20-diphenylporphyrin (**11**) (0.050 g, 0.080 mmol) was dissolved in CH_2Cl_2 (3 mL) and TBAF (0.162 mL, 0.162 mmol) was added to the solution. After 30 min, CH_3CO_2H (13 μL) and CH_3OH (4 mL) were added to the reaction. The mixture was filtered after 30 min and the solid product was washed with methanol to provide **13** (27 mg, 65%) as a purple solid: m.p.> 300 °C; R_f: 0.62 (EtOAc/hexanes 1:10); IR (ATR, cm^{-1}) ν 3265, 2968, 2085, 1806, 1593, 1560, 1475, 1442, 1401, 1347, 1260, 1199, 1159, 1093, 1064, 1028, 969, 913, 877, 794, 786, 749, 732, 716, 699, 676, 659; UV/Vis ($CHCl_3$) λ_{max} (log ε): 427 (5.32), 531 (4.02), 571 (4.24), 608 (3.64), 670 (3.83) nm; ^1H NMR (400 MHz, $CDCl_3$) δ 9.59 (d, *J* = 4.4 Hz, 4H, β-H), 8.79 (d, *J* = 3.9 Hz, 4H, β-H), 8.11 (d, *J* = 7.3 Hz, 4H, Ph-H), 7.79–7.68 (m, 6H, Ph-H), 4.14 (s, 2H, C≡CH), −2.40 (br s, 2H, NH); HRMS (ESI): *m/z* calcd for $C_{36}H_{23}N_4$ $[M+H]^+$ 511.1917, found 511.1920.

*4.11. 5,15-Diethynyl-10,20-diphenylporphyrinato-zinc(II) (**14**)*

5,15-Bis(trimethylsilylethynyl)-10,20-diphenylporphyrinato-zinc(II) (**12**) (0.086 mmol) was dissolved in CH_2Cl_2 (4 mL) and TBAF (0.175 mL, 0.175 mmol) was added to the solution. After 30 min, CH_3CO_2H (15 μL) and CH_3OH (5 mL) were added to the reaction. The mixture was filtered after 30 min and the solid product was washed with methanol to provide **14** (34 mg, 68%) as a purple solid: m.p.> 300 °C; R_f: 0.78 (EtOAc/hexanes 1:3); IR (ATR, cm^{-1}) ν 3259, 2090, 1803, 1595, 1498, 1441, 1342, 1308, 1262, 1229, 1211, 1173, 1066, 1003, 995, 969, 934, 915, 847, 828, 791, 750, 737, 712, 699, 673, 663, 654; UV/Vis ($CHCl_3$) λ_{max} (log ε): 430 (5.29), 575 (3.90), 622 (4.11) nm; ^1H NMR (400 MHz, d_8-THF) δ 9.55 (d, *J* = 4.6 Hz, 4H, β-H), 8.72 (d, *J* = 4.6 Hz, 4H, β-H), 8.06 (d, *J* = 7.6 Hz, 4H, Ph-H), 7.60–7.70 (m, 6H, Ph-H), 4.52 (s, 2H, C≡CH); HRMS (ESI): *m/z* calcd for $C_{36}H_{21}N_4Zn$ $[M+H]^+$ 573.1052, found 573.1055.

*4.12. Dyad **15***

10-(4-Bromophenyl)-5,15-diphenylcorrole-copper(III) (**3**) (93 mg, 0.14 mmol) and 5-ethynyl-10,20-diphenylporphyrin (**8**) (68 mg, 0.14 mmol) were dissolved in Et_3N/toluene (1:3, 60 mL) and the mixture was deoxygenated. $AsPh_3$ (0.030 g, 0.120 mmol) and $Pd_2(dba)_3$ (0.012 g, 0.060 mmol) were added to the reaction and the mixture was stirred for 12 h at 40 °C. The reaction was quenched with H_2O (10 mL). The aqueous phase was extracted with $CHCl_3$ (3 × 10 mL). The solvent was removed under reduced pressure. The crude product was purified by flash column chromatography ($CHCl_3$/hexanes 1:1) to provide **15** (96 mg, 64%) as a purple solid: m.p.> 300 °C; R_f: 0.80 ($CHCl_3$/hexanes 1:1); IR (ATR, cm^{-1}) ν 3646, 3630, 2957, 2925, 2855, 2361, 1717, 1668, 1648, 1430, 1390, 1363, 1314, 1247, 1231, 1215, 1197, 1158, 1120, 1103, 1072, 1054, 1026, 972, 961, 931, 885, 860, 825, 809, 775, 769, 755, 740, 723, 700, 658, 652; UV/Vis ($CHCl_3$) λ_{max} (log ε): 413 (4.13), 508 (3.14), 539 (2.62), 581 (2.68), 649 (1.84) nm; ^1H NMR (400 MHz, $CDCl_3$) δ 10.32 (s, 1H, meso-H), 9.39 (d, *J* = 4.6 Hz, 2H, porp β-H), 9.30 (d, *J* = 4.8 Hz, 2H, porp β-H), 9.10 (d, *J* = 4.8 Hz, 2H, porp β-H), 9.07 (d, *J* = 4.6 Hz, 2H, porp β-H), 8.30–8.26 (m, 4H, Ph-H), 7.87–7.80 (m, 6H, Ph-H), 7.79–7.75 (m, 4H, cor β-H), 7.60–7.52 (m, 4H, cor β-H), 7.36–7.29 (m, 6H, Ph-H), 7.20–7.14 (m, 8H, Ph-H), −3.03 (br s, 2H, NH); ^{13}C NMR (100 MHz, $CDCl_3$) δ 169.4, 150.5, 140.7, 135.7, 133.2, 131.4, 130.3, 128.8, 128.2, 127.2, 126.5, 125.5, 124.9, 122.7, 121.5, 93.0, 88.6; HRMS (ESI): *m/z* calcd for $C_{71}H_{44}CuN_8$ $[M+H]^+$ 1071.2979, found 1071.2892.

*4.13. Dyad **16***

A solution of 10-(4-Bromophenyl)-,15-diphenylcorrole-copper(III) (**3**) (0.055 g, 0.0826 mmol), 5-ethynyl-10,20-diphenylporphyrinato-zinc(II) (**9**) (0.050 g, 0.091 mmol), $PdCl_2(PPh_3)_2$ (0.003 g, 0.0041 mmol) and CuI (0.001 g, 0.0041 mmol) in 5 mL of Et_3N (5 mL) and toluene (3 mL) was deoxygenated and stirred at 40 °C under N_2 atmosphere. After 8 h, the mixture was cooled to room temperature and H_2O (5 mL) was added. The aqueous phase was extracted with CH_2Cl_2 (3 × 5 mL). The solvent was removed under reduced pressure. The crude product was purified by flash column chromatography ($CHCl_3$/hexanes 1:1) to provide **16** (64 mg, 68%) as a purple solid: m.p.> 300 °C; R_f: 0.83 ($CHCl_3$/hexanes 1:1); IR (ATR, cm^{-1}) ν 2957, 2924, 2853, 1731, 1600, 1492, 1461, 1377, 1272, 1210, 1122, 1093, 1073, 1044, 1002, 993, 877, 847, 820, 793, 781, 749, 21, 699, 668, 656; UV/Vis ($CHCl_3$) λ_{max} (log ε): 418 (4.47), 548 (3.36) nm; ^1H NMR (400 MHz, $CDCl_3$) δ 10.26 (s, 1H, meso-H), 9.56 (d, *J* = 4.6 Hz, 2H, porp β-H), 9.38 (d, *J* = 4.5 Hz, 2H, porp β-H), 9.08–9.04 (m, 4H, porp β-H), 8.22 (br s, 4H, Ph-H), 7.80–7.75 (m, 6H, Ph-H), 7.74–7.69 (m, 4H, cor β-H), 7.55–7.51 (m, 4H, cor β-H), 7.30–7.20 (m, 12H, Ph-H), 7.19–7.10 (m, 8H, Ph-H); ^{13}C NMR (100 MHz, $CDCl_3$) δ 169.5, 151.5, 145.4, 140.7, 135.7, 135.6, 134.5, 132.4, 131.4, 128.8, 128.3, 128.2, 126.6, 125.5, 124.9, 93.4, 92.0; HRMS (ESI): *m/z* calcd for $C_{71}H_{42}CuN_8Zn$ $[M+H]^+$ 1133.2114, found 1133.2076.

*4.14. Triad **17***

10-(4-Bromophenyl)-5,15-diphenylcorrole-copper(III) (**3**) (186 mg, 0.280 mmol) and 5,15-dibromo-10,20-diphenylporphyrin (**13**) (72 mg, 0.140 mmol) were dissolved in Et_3N/toluene (1:3, 80 mL) and the mixture was deoxygenated. $AsPh_3$ (0.060 g, 0.240 mmol) and $Pd_2(bda)_3$ (0.024 g, 0.120 mmol) were added to the reaction and the mixture was stirred for 12 h at 40 °C under N_2 atmosphere. The reaction was quenched with H_2O (10 mL). The aqueous phase was extracted with $CHCl_3$ (3 × 10 mL). The solvent was removed under reduced pressure. The crude product was purified by flash column chromatography ($CHCl_3$/hexanes 1:1) to provide **17** (113 mg, 48%) as a purple solid: m.p.> 300 °C; R_f: 0.71 ($CHCl_3$/hexanes 1:1); IR (ATR, cm^{-1}) ν 2963, 2925, 2850, 2358, 2328, 1717, 1679, 1653, 1559, 1507, 1457, 1376, 1259, 1215, 1160, 1106, 1072, 1011, 885, 799, 712, 668; UV/Vis ($CHCl_3$) λ_{max} (log ε): 427 (4.83), 532 (3.76), 571 (3.91), 609 (3.46), 670 (3.58); ^1H NMR (400 MHz, d_8-THF) δ 9.56 (d, *J* = 4.6 Hz, 4H, porp β-H), 8.74 (d, *J* = 5.0 Hz, 4H, porp β-H), 8.12–8.07 (m, 4H, Ph-H), 7.90–7.85 (m, 4H, cor β-H), 7.74–7.70 (m, 6H, cor β-H), 7.68–7.62 (m, 8H, Ph-H),

Please cite this article in press as: B. Temelli, et al., Ethynyl-bridged porphyrin-corrole dyads and triads: Synthesis, properties and DFT calculations, Tetrahedron (2018), https://doi.org/10.1016/j.tet.2018.07.007

7.60–7.57 (m, 4H, cor β-H), 7.54–7.51 (m, 4H, cor β-H), 7.50–7.45 (m, 8H, 4 cor β-H, 4 Ph-H), 7.45–7.42 (m, 8H, Ph-H), 7.27–7.24 (m, 4H, Ph-H), 7.15–7.12 (m, 4H, Ph-H), −2.35 (br s, 2H, NH); ^{13}C NMR (100 MHz, $CDCl_3$) δ 169.6, 140.8, 135.6, 131.4, 128.8, 128.3, 125.5, 124.9, 121.6, 93.5, 89.9; HRMS (ESI): *m/z* calcd for $C_{110}H_{65}Cu_2N_{12}$ $[M+H]^+$ 1679.4047, found 1679.4094.

4.15. Triad **18**

A solution of 10-(4-bromophenyl)-5,15-diphenylcorrole-copper(III) (**3**) (0.182 g, 0.273 mmol), 5,15-diethynyl-10,20-diphenylporphyrinato-zinc(II) (**14**) (0.050 g, 0.091 mmol), $PdCl_2(PPh_3)_2$ (0.007 g, 0.0091 mmol) and CuI (0.002 g, 0.0091 mmol) in 7 mL of Et_3N and 5 mL of toluene was deoxygenated and stirred at 40 °C under N_2 atmosphere. After 8 h, the mixture was cooled to room temperature and H_2O (10 mL) was added. The aqueous phase was extracted with CH_2Cl_2 (3 × 10 mL). The solvent was removed under reduced pressure. The crude product was purified by flash column chromatography ($CHCl_3$/hexanes 1:1) to provide **18** (64 mg, 40%) as a purple solid: m.p.> 300 °C; R_f: 0.80 ($CHCl_3$/hexanes 1:1); IR (ATR, cm^{-1}) ν 3375, 3053, 2920, 2850, 1682, 1588, 1516, 1492, 1422, 1366, 1339, 1310, 1250, 1190, 1108, 1070, 1052, 1020, 1009, 982, 898, 874, 831, 811, 789, 758, 732, 707, 674; UV/Vis ($CHCl_3$) λ_{max} (log ε): 441 (4.59), 575 (3.76), 531 (3.65), 622 (3.90); ^{1}H NMR (400 MHz, d_8-THF) δ 9.55 (d, *J* = 4.6 Hz, 4H, porp β-H), 8.73 (d, *J* = 4.5 Hz, 4H, porp β-H), 8.07 (d, *J* = 6.5 Hz, 4H, Ph-H), 7.85 (br s, 2H, cor β-H), 7.79 (s, 2H, cor β-H), 7.72–7.60 (m, 14H, Ph-H), 7.59–7.55 (m, 4H, cor β-H), 7.52–7.49 (m, 4H, cor β-H), 7.49–7.45 (m, 8H, 4 cor β-H, 4 Ph-H), 7.38–7.44 (m, 8H, Ph-H), 7.24 (br s, 4H, Ph-H), 7.15–7.10 (m, 4H, Ph-H); ^{13}C NMR (100 MHz, $CDCl_3$) δ 169.7, 141.0, 140.8, 135.8, 128.4, 128.2, 125.5, 96.8, 89.2; HRMS (ESI): *m/z* calcd for $C_{110}H_{63}Cu_2N_{12}Zn$ $[M+H]^+$ 1741.3177, found 1741.2995.

4.16. Computational methods

Computational studies were performed using B3LYP [23] hybrid functional in combination with the 6-311G(d,p) [24] basis set. Vertical excitation energies were computed by means of time-dependent density functional theory (TD-DFT) calculations based on the optimized geometries. The lowest 100 vertical excitation energy states were considered. All DFT and TD-DFT calculations in this study were performed using the Gaussian 09 software [25]. For the visualization of the optimized geometries and the molecular orbitals, the GaussView [26] software was used. The Mulliken Population Analysis (MPA) of the molecular orbitals was performed using the GaussSum package [27].

Acknowledgements

The authors thank Hacettepe University (BAP project 014 09 601 002-723) and The Scientific and Technological Research Council of Turkey (project number: 115Z886) for financial support.

Appendix A. Supplementary data

Supplementary data associated with this article can be found in the online version, at https://doi.org/10.1016/j.tet.2018.07.007. These data include MOL files and InChiKeys of the most important compounds described in this article.

References

[1] (a) L.R. Milgrom, The Colours of Life: an Introduction to the Chemistry of Porphyrins and Related Compounds, Oxford University Press, New York, 1997;
(b) K.M. Kadish, K.M. Smith, R. Guilard, The Porphyrin Handbook, vols. 1–20, Academic Press, San Diego, 2000.

[2] (a) J.-H. Chou, M.E. Kosal, H.S. Nalwa, N.A. Rakow, K.S. Suslick, in: K. Kadish, K. Smith, R. Guilard (Eds.), Porphyrin Handbook, vol. 6, Academic Press, New York, 2000, pp. 43–131;
(b) article in press: S. Shao, et al., Metalloporphyrin nanoparticles: coordinating diverse theranostic functions Coord. Chem. Rev. (2017) https://doi.org/10.1016/j.ccr.2017.09.002.

[3] D. Kim, Multiporphyrin Arrays: Fundamentals and Applications, Pan Stanford, Singapore, 2012.

[4] (a) R. Paolesse, R.K. Pandey, T.P. Forsyth, L. Jaquinod, K.R. Gerzevske, D.J. Nurco, M.O. Senge, S. Licoccia, T. Boschi, K.M. Smith, J. Am. Chem. Soc. 118 (1996) 3869;
(b) R. Guilard, F. Jérôme, C.P. Gros, J.-M. Barbe, Z. Ou, J. Shao, K.M.C.R. Kadish, Acad. Sci. Ser. IIc: Chim. 4 (2001) 245;
(c) R. Guilard, F. Burdet, J.-M. Barbe, C.P. Gros, E. Espinosa, J. Shao, Z. Ou, R. Zhan, K.M. Kadish, Inorg. Chem. 44 (2005) 3972;
(d) L. Flamigni, B. Ventura, M. Tasior, D.T. Gryko, Inorg. Chim. Acta. 360 (2007) 803;
(e) T.H. Ngo, F. Nastasi, F. Puntoriero, S. Campagna, W. Dehaen, W. Maes, Eur. J. Org. Chem. (2012) 5605;
(f) T.H. Ngo, D. Zieba, W.A. Webre, G.N. Lim, P.A. Karr, S. Kord, S. Jin, K. Ariga, M. Galli, S. Goldup, J.P. Hill, F. D'Souza, Chem. Eur. J. 22 (2016) 1301;
(g) V. Nikolaou, K. Karikis, Y. Farré, G. Charalambidis, F. Odobel, A.G. Coutsolelos, Dalton Trans. 44 (2015) 13473;
(h) M. Murugavel, R.V.R. Reddy, J. Sankar, RSC Adv. 4 (2014) 13669;
(i) C. Chen, Y.-Z. Zhu, Q.-J. Fan, H.-B. Song, J.-Y. Zheng, Chem. Lett. 42 (2013) 936;
(j) S. Hiroto, I. Hisaki, H. Shinokubo, A. Osuka, Angew. Chem. Int. Ed. 44 (2005) 6763.

[5] (a) C.B. KC, G.N. Lim, F. D'Souza, Nanoscale 7 (2015) 6813;
(b) A.M.V.M. Pereira, A.R.M. Soares, A. Hausmann, M.G.P.M.S. Neves, A.C. Tomé, A.M.S. Silva, J.A.S. Cavaleiro, D.M. Guldi, T. Torres, Phys. Chem. Chem. Phys. 13 (2011) 11858;
(c) A.R.M. Soares, V.M. Martinez-Diaz, A. Bruckner, A.M.V.M. Pereira, J.P.C. Tomé, C.M.A. Alonso, M.A.F. Faustino, M.G.P.M.S. Neves, A.C. Tomé, A.M.S. Silva, J.A.S. Cavaleiro, T. Torres, D.M. Guldi, Org. Lett. 9 (2007) 1557.

[6] Y. Inokuma, S. Hayashi, A. Osuka, Chem. Lett. 38 (2009) 206.

[7] (a) C.Y. Le, J.T. Hupp, Langmuir 26 (2010) 3760;
(b) C. Jiao, L. Zhu, J. Wu, Chem. Eur. J. 17 (2011) 6610;
(c) T.K. Khan, M. Ravikanth, Tetrahedron 68 (2012) 830;
(d) M.J. Leonardi, M.R. Topka, P.H. Dinolfo, Inorg. Chem. 51 (2012) 13114;
(e) B. Brizet, A. Eggenspiller, C.P. Gros, J.-M. Barbe, C. Goze, F. Denat, P.D. Harvey, J. Org. Chem. 77 (2012) 3646;
(f) Q.-Q. Hu, Y.-Z. Zhu, S.-C. Zhang, Y.-Z. Tong, J.-Y. Zheng, Dalton Trans. 44 (2015) 15523.

[8] (a) T. Tanaka, N. Aratani, J.M. Lim, K.S. Kim, D. Kim, A. Osuka, Chem. Sci. 2 (2011) 1414;
(b) H. Mori, T. Tanaka, S. Lee, J.M. Lim, D. Kim, A. Osuka, J. Am. Chem. Soc. 137 (2015) 2097.

[9] (a) J.F.B. Barata, M.G.P.M.S. Neves, M.A.F. Faustino, A.C. Tomé, J.A.S. Cavaleiro, Chem. Rev. 117 (2017) 3192;
(b) R. Orlowski, D. Gryko, D.T. Gryko, Chem. Rev. 117 (2017) 3102;
(c) I. Aviv, Z. Gross, Chem. Commun. (2007) 1987.

[10] B. Temelli, O. Ozasik, D. Yüksel, Eur. J. Org. Chem. (2017) 4905.

[11] B. Temelli, H. Kalkan, Beilstein J. Org. Chem. 14 (2018) 187.

[12] B. Koszarna, D.T. Gryko, J. Org. Chem. 71 (2006) 3707.

[13] M. Murugavel, R.V.R. Reddy, D. Dey, J. Sankar, Chem. Eur. J. 21 (2015) 14280.

[14] I. Luobeznova, L. Simkhovich, I. Goldberg, Z. Gross, Eur. J. Inorg. Chem. 8 (2004) 1724.

[15] C. Brückner, R.P. Briñas, J.A. Krause Bauer, Inorg. Chem. 42 (2003) 4495.

[16] C.M. Lemon, M. Huynh, A.G. Maher, B.L. Anderson, E.D. Bloch, D.C. Powers, D.G. Nocera, Angew. Chem. Int. Ed. 55 (2016) 2176.

[17] A.B. Alemayehu, L.K. Hansen, A. Ghosh, Inorg. Chem. 49 (2010) 7608.

[18] K. Pierloot, H. Zhao, S. Vancoillie, Inorg. Chem. 49 (2010) 10316.

[19] W. Sinha, M.G. Sommer, N. Deibel, F. Ehret, M. Bauer, B. Sarkar, S. Kar, Angew. Chem. Int. Ed. 54 (2015) 13769.

[20] B.J. Littler, M.A. Miller, C.-H. Hung, R.W. Wagner, D.F. O'Shea, P.D. Boyle, J.S. Lindsey, J. Org. Chem. 64 (1999) 1391.

[21] S.G. DiMagno, V.S.-Y. Lin, M.J. Therien, J. Org. Chem. 58 (1993) 5983.

[22] C. Liu, D.-M. Shen, Q.-Y. Chen, Chem. Commun. (2006) 770.

[23] (a) A.D. Becke, J. Chem. Phys. 98 (1993) 5648;
(b) C. Lee, W. Yang, R.G. Parr, Phys. Rev. B 37 (1988) 785.

[24] (a) A.D. McLean, G.S. Chandler, J. Chem. Phys. 72 (1980) 5639;
(b) K. Raghavachari, J.S. Binkley, R. Seeger, J.A. Pople, J. Chem. Phys. 72 (1980) 650;
(c) A.J.H. Wachters, J. Chem. Phys. 52 (1970) 1033;
(d) P.J. Hay, J. Chem. Phys. 66 (1977) 4377.

[25] M.J. Frisch, G.W. Trucks, H.B. Schlegel, G.E. Scuseria, M.A. Robb, J.R. Cheeseman, G. Scalmani, V. Barone, B. Mennucci, G.A. Petersson, H. Nakatsuji, M. Caricato, X. Li, H.P. Hratchian, A.F. Izmaylov, J. Bloino, G. Zheng, J.L. Sonnenberg, M. Hada, M. Ehara, K. Toyota, R. Fukuda, J. Hasegawa, M. Ishida, T. Nakajima, Y. Honda, O. Kitao, H. Nakai, T. Vreven, J.A. Montgomery Jr., J.E. Peralta, F. Ogliaro, M. Bearpark, J.J. Heyd, E. Brothers, K.N. Kudin, V.N. Staroverov, T. Keith, R. Kobayashi, J. Normand, K. Raghavachari, A. Rendell, J.C. Burant, S.S. Iyengar, J. Tomasi, M. Cossi,

Please cite this article in press as: B. Temelli, et al., Ethynyl-bridged porphyrin-corrole dyads and triads: Synthesis, properties and DFT calculations, Tetrahedron (2018), https://doi.org/10.1016/j.tet.2018.07.007

N. Rega, J.M. Millam, M. Klene, J.E. Knox, J.B. Cross, V. Bakken, C. Adamo, J. Jaramillo, R. Gomperts, R.E. Stratmann, O. Yazyev, A.J. Austin, R. Cammi, C. Pomelli, J.W. Ochterski, R.L. Martin, K. Morokuma, V.G. Zakrzewski, G.A. Voth, P. Salvador, J.J. Dannenberg, S. Dapprich, A.D. Daniels, O. Farkas, J.B. Foresman, J.V. Ortiz, J. Cioslowski, D.J. Fox, Gaussian 09, Revision C.01, Gaussian, Inc., Wallingford CT, 2010.

[26] R.D. Dennington II, T.A. Keith, J.M. Millam, GaussView, Semichem, Inc., Wallingford, CT, 2008, 5.0.8. .

[27] N.M. O'Boyle, A.L. Tenderholt, K.M. Langner, J. Comput. Chem. 29 (2008) 839.

Please cite this article in press as: B. Temelli, et al., Ethynyl-bridged porphyrin-corrole dyads and triads: Synthesis, properties and DFT calculations, Tetrahedron (2018), https://doi.org/10.1016/j.tet.2018.07.007